

Optimizing the performance of nickel-like collisionally pumped x-ray lasers. III. Exploding foil lasers for the wavelength range below 50 Å

G. J. Pert

Physics Department, University of York, Heslington, York, YO10 5DD, United Kingdom

(Received 5 February 2007; published 15 June 2007)

In previous work, it was found that heat conduction limited the development of laser action at wavelengths below 50 Å. In this paper, we discuss the use of thin foils to limit these effects, and generate a high-density and -temperature plasma with low refractive index gradient. By using a relatively short (~ 100 ps) first pulse and short (~ 1 ps) second, it is shown that effective high-gain systems may be developed.

DOI: [10.1103/PhysRevA.75.063814](https://doi.org/10.1103/PhysRevA.75.063814)

PACS number(s): 42.55.Vc, 32.30.Rj, 42.60.By, 52.50.Jm

I. INTRODUCTION

This work is the concluding part of a series of papers surveying the operation of Ni-like collisionally pumped x-ray lasers heated by multiple pulse irradiation. The previous parts have examined systems in the wavelength ranges >100 Å [1] (paper I) and $100\text{--}50$ Å [2] (paper II), in which the plasma is produced from a slab target. However, as we found in II, the high temperature required for ionization generates a substantial body of plasma heated by conduction. In this paper we limit the plasma mass by using thin foil targets.

Foil targets were successfully used in the series of experiments at Livermore Laboratory in the 1980s commencing with the first unequivocal demonstration of soft x-ray laser action [3]. After initially using Ne-like ions, the authors demonstrated laser action in Ni-like ions: europium at 66 and 70 Å [4], ytterbium (50 Å) [5], tantalum (45 Å) [6], tungsten (43 Å) [6], and gold (36 Å) [7]. All these experiments were performed using the NOVA laser at Livermore, which was at that time the only one capable of delivering the large pump energies required. The gain was weak ($\sim 2\text{ cm}^{-1}$) and the lasers could not reach saturation. As a result the exploding foil approach to x-ray lasers fell into disfavor as designs based on slab targets using multiple pulses overcame the limitations of this simpler approach.

However, x-ray lasers based on slab targets have proved unable to generate the shortest wavelengths. To date, the shortest saturated wavelength achieved using a slab was obtained with dysprosium (59 Å) at the Rutherford laboratory [8]. Pump energy limitations have prevented further extension to shorter wavelengths. In this paper, we will examine the potential for foils using two-sided double pump pulses to ease this restriction. The pump will comprise a relatively short (~ 100 ps) first pulse (prepulse) to establish the hydrodynamic expansion and ionize the plasma, followed at its termination by a short (~ 1 ps) second (main) pulse to further heat the plasma. The prepulse energy will be much larger than that of the main pulse. The wavelength used for both pulses will be the second harmonic of Nd glass (0.53 μm).

The paper will present the results in two parts. The first will give a series of estimates based on analytic scalings to identify the principle parameters. The second part will consist of a set of simulation experiments to confirm the basic picture using the EHYBRID and RAYTRACE codes described in paper II.

As in the earlier papers, we will use relatively simple, but well-established, models of complex processes, such as thermal conduction and ionization, in both the analytic and simulation calculations. As a consequence the results are not accurate enough to be interpreted as exact representations of an actual experiment. However, they are adequate to enable us to achieve the key aim of this work, namely, to identify the principal design constraints and the scalings of this type of laser.

II. ANALYTIC ESTIMATES

A. Ionization and inversion

The primary criterion determining the performance of these lasers is to ensure that the ionization at the end of the plasma formation (prepulse) has the correct value to allow population inversion to be developed in the Ni-like ion. Secondary, but also important, is to ensure that the plasma density profile does not have a steep gradient in the region where strong gain is to be developed. As we showed in our previous work paper II, the ionization determines the temperature that must be achieved in the prepulse plasma before the main pulse is applied. The scaling of this value with atomic number Z leads to rapid increases in the laser irradiation needed at the surface of a slab target. It was shown in the earlier work that the electron temperature required scaled approximately as $T_e \sim Z^{1/2}$.

It was also found that the time taken for the required ionization to be established increased rapidly for atomic numbers above about 70 (Fig. 1). We note that the time required scales with electron density n_e approximately as n_e^{-1} . It can be seen that for high atomic number we must use high density, high temperature, or long ionizing pulse. Since the latter two options both require larger prepulse energies, the former is preferable.

Turning now to the generation of the population inversion and gain, we show in Fig. 2 the inversion plot for tantalum ($Z=73$). The quantities plotted are the same as those in paper II, namely, the steady-state inversion density normalized to the ground-state density of the Ni-like ion, and the gain parameter defined as the former multiplied by a reduced electron density. For electron densities below 10^{21} cm^{-3} , the inversion fraction scales roughly linearly with electron density, as the upward transitions are collisional and balanced by downward radiative transitions: therefore in this region the

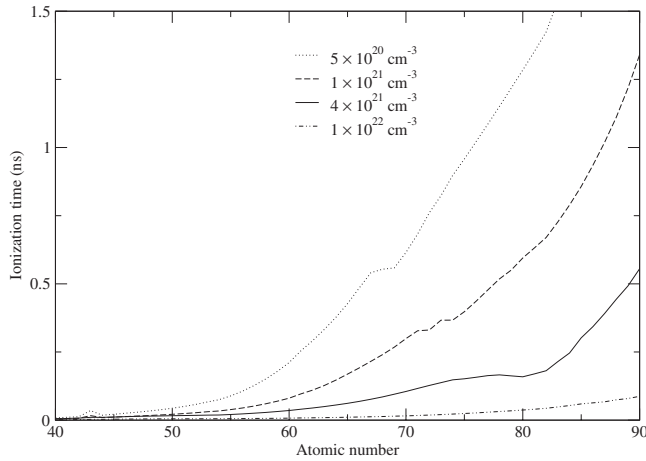


FIG. 1. Time taken to achieve Cu-like ionization in plasma at the equilibrium ionization temperature for the Ni-like ion at different densities.

gain scales approximately quadratically with electron density. As collisional decay becomes important near the maximum of the inversion fraction, the gain scaling becomes nearly linear. It can be clearly seen from Fig. 2 that the gain benefits from working at a high density. It suggests that we should endeavour to generate Ni-like plasma in the appropriate elements at density $\sim 10^{22} \text{ cm}^{-3}$.

We observe from Fig. 2 that the inversion fraction and gain parameter are relatively insensitive to increases in temperature above about 1.5 keV. The same feature may also be seen in the plots for dysprosium in paper II. This arises from a competition between the increased excitation and ionization rates as the temperature increases. The former increases the inversion, but the latter decreases the overall population in the Ni-like ion stage. The significance of this observation is that there is relatively little to be gained by further increases in temperature beyond a certain limit, and that consequently the main pulse energy can be limited.

B. Plasma from slabs

In our earlier paper II we reviewed the properties of the plasma formed by ablation from the surface of solid slab

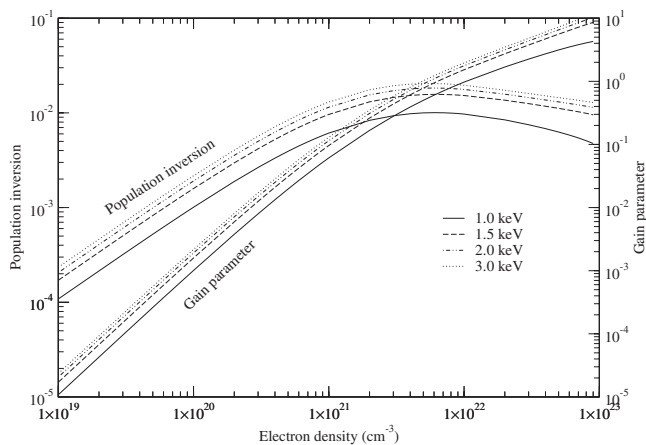


FIG. 2. Normalized inversion density and gain parameter as functions of electron density at various electron temperatures for the line at 45 \AA in tantalum.

targets. For the conditions required by x-ray lasers, we found that the plasma was described by a combination of an expansion fan and an upstream thermal conduction zone. As the temperature increased to provide the ionization for operation at shorter wavelengths, the upstream zone dominated the flow in terms of the mass and plasma energy. From this analysis we obtained a set of empirical relations for the absorption electron density and laser irradiance required to generate the necessary ionization temperature as a function of the atomic number Z , wavelength λ , and pulse duration τ . These scaling relations are valid in the ranges $60 < Z < 90$, $100 < \tau < 600 \text{ ps}$ and $0.5 < \lambda < 1.0 \text{ \mu m}$, appropriate to our current study. We will not repeat these here, but refer to paper II for the values.

The mass and energy of the upstream conduction zone can be expressed in terms of simple empirical scalings given in paper II. The characteristic time for the creation and relaxation of the conduction zone is calculated from the time taken for a fluid element to pass through the zone [9], which is easily shown to be

$$\tau_R = \frac{M}{\dot{\mu}}, \quad (1)$$

where M is the area mass density of the zone and $\dot{\mu}$ the mass flux into the expansion fan, i.e., the ablation rate. The ablation rate depends on whether the flow is of the deflagration or self-regulating type, i.e., whether the absorption is local at critical density or global determined by inverse bremsstrahlung. Hence, using the scaling relations given previously, the limiting values for this time are

$$\tau_R \text{ (ps)} \approx \begin{cases} 1.18 \times 10^{-9} Z^{13/2} [\lambda \text{ (\mu m)}]^2, \\ 9.10 \times 10^{-7} Z^{9/2} [\lambda \text{ (\mu m)}][\tau \text{ (ps)}]^{1/2} \end{cases} \quad (2)$$

for the deflagration and self-regulating pictures, respectively.

Since the total mass ablated into the ablation fan is approximately $\dot{\mu}\tau$, where τ is the pulse duration, it can be seen from Eq. (1) that the ratio of the relaxation time to the pulse duration is approximately equal to that of the upstream to downstream mass. Thus, if the upstream mass is large, the thermal conduction zone may not be fully developed into its steady-state form before the pulse terminates. We may note that in some of the cases studied in paper II this condition was not satisfied.

C. Exploding foils

Thin foils illuminated on two sides by identical laser beams disassemble rapidly and symmetrically about their central plane. The behavior of these targets was investigated in some detail by London and Rosen [10]. Comparing the self-similar model with LASNEX simulations, it was shown that, once the burnthrough was complete, the simple model provided a reasonably realistic picture of the subsequent expansion. This is in keeping with Nemchinov's hypothesis [11,12] that the hydrodynamic limit of the expansion of infinitesimally small bodies is a self-similar expansion of the appropriate type. Since thermal conduction is strong in these plasmas, the isothermal description is appropriate in which

the density distribution is Gaussian with appropriate mass. Thus, for a one-dimensional foil of mass M per unit area, the density

$$\rho = \frac{M}{\sqrt{\pi}x_1} \exp\left(-\frac{x^2}{x_1^2}\right), \quad (3)$$

where x is the distance from the center of mass and x_1 is the $1/e$ width of the profile. Calculating the total energy as the sum of the thermal and kinetic terms, respectively, we obtain

$$E = M \left[\frac{3}{4} x_1 \frac{d^2 x_1}{dt^2} + \frac{1}{4} \left(\frac{dx_1}{dt} \right)^2 \right]. \quad (4)$$

Solving for the case when the energy increases as a power of time $E \propto t^n$ and $x_1 = \dot{x}_1 = 0$ at $t=0$, we obtain

$$x_1 = \sqrt{\left(\frac{8}{(n+2)(2n+1)} \frac{E}{M} \right)} t. \quad (5)$$

The kinetic and thermal energies are easily shown to be in the constant ratio $3n/(n+2)$. Noting that this ratio increases as n increases may suggest that we should use the rapidly rising edge of the prepulse. However, remembering that the pulse also has a tail of equal or greater energy erodes any such advantage. When the source has constant power, Φ' and $n=1$, the two energy components are equal. In this case, the scale length increases as

$$x_1 = \sqrt{\left(\frac{8 \Phi'}{9 M} \right)} t^{3/2} \quad (6)$$

and the central density decreases as

$$\rho_0 = \sqrt{\left(\frac{9M}{8\pi E} \right)} \frac{M}{t}. \quad (7)$$

Thus, for a given mass the temperature and central density are determined by the total pulse energy and time.

D. Burnthrough

For these designs to work well, it is essential that the density distribution be smooth at the origin (approximately Gaussian), be reasonably wide, and that the temperature be reasonably uniform. It is therefore desirable to ensure that the disassembling foil have time to assume an approximate similarity profile with the appropriate central density. It is difficult to accurately estimate this time for foils. We can identify lower bounds by considering the early development involving the competing effects of the inward propagation of the heat front and the leading characteristic [13], which determine the onset of the outward flow as the foil starts to expand. For a $100 \mu\text{g}/\text{cm}^2$ tantalum foil these are 1.6 and 3.5 ps, respectively. The onset of thermally driven hydrodynamic motion is therefore very rapid.

An upper bound is set by the time that the ablation causes the central density to reach the critical value [10]. This time is approximately given by $M/\dot{\mu}$, equal to the thermal layer steady-state relaxation time, Eq. (1): a time in this case of 330 ps. However, this model takes no account of the expansion associated with the heat front. On the other hand, the

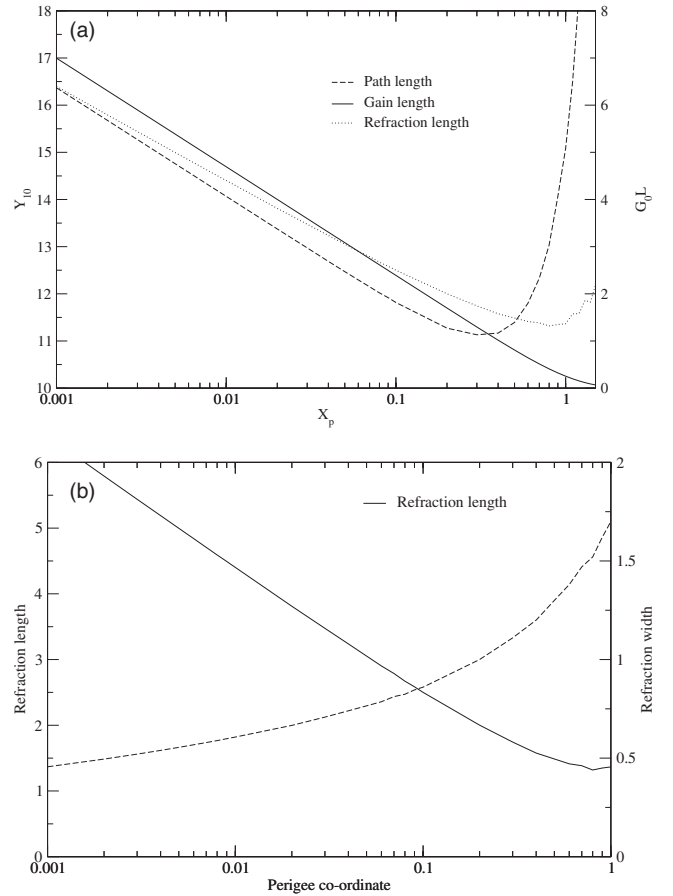


FIG. 3. Path length and gain length at $X=10$ (a) and the refraction length as function of ray perigee position X_p (b).

similarity model, which includes complete thermal transport, gives a lower bound and predicts a time of 90 ps [Eq. (7)]. The actual time for the central density to become critical will lie somewhere between these two limits. Simulation gives a time of about 150 ps to reach critical density under these conditions.

Although the critical density for $0.53 \mu\text{m}$ radiation is $4 \times 10^{21} \text{ cm}^{-3}$, we would prefer to use a higher density to improve the gain. From Fig. 2, we can see that an increase in density to 10^{22} cm^{-3} gives a factor of 3 improvement in gain. We may note that the ionization time to reach the Cu-like stage is about 20 ps (Fig. 1). This suggests that an appropriate pulse length for our purpose may be about 100 ps.

E. Refraction

The role of refraction in exploding foil x-ray lasers was considered in detail by London [14] using a parabolic density profile. The limitation of the effective gain length in slab targets by refraction was briefly discussed in paper I. In this section we briefly discuss refraction in a Gaussian density profile.

We first develop a simple two-dimensional model for rays whose perigee is at some point x_p in a Gaussian density profile of $1/e$ width x_1 , Eq. (5). In the paraxial limit $n_c \gg n_0$, we define two reduced scale coordinates $X=x/x_1$ and

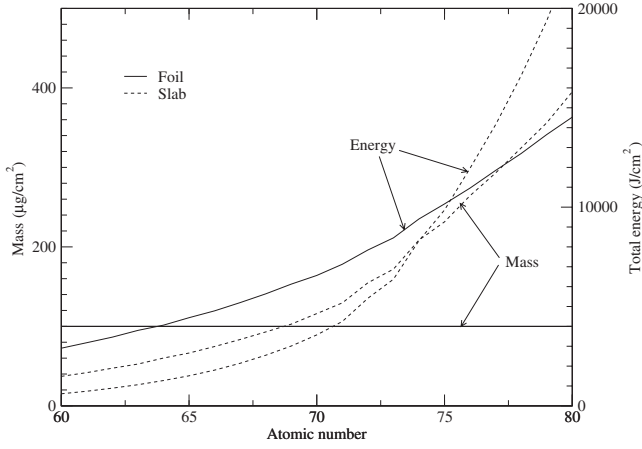


FIG. 4. Comparison of the mass and energy for a 100 μg foil and a slab heated in the self-regulating mode by a pulse of wavelength 0.5 μm and pulse duration 100 ps.

$Y = \sqrt{n_0/n_c}(y/x_1)$ where x and y are parallel and perpendicular to the density gradient, respectively, n_0 is the electron density at the central maximum, and n_c is the critical density for the x-ray radiation. The equation of the ray starting from its perigee, i.e., parallel to the axis, at X_p is then given by

$$\frac{dY}{dX} = [\exp(-X_p^2) - \exp(-X^2)]^{-1/2}. \quad (8)$$

If the perigee is at the center of the profile, $X_p=0$, the ray continues along the axis. Generally, however, the ray is deflected and its path can be determined by quadrature. In the neighborhood of the turning point [$(X^2 - X_p^2) \ll 1$],

$$\begin{aligned} Y &= \exp\left(\frac{1}{2}X_p^2\right) \operatorname{arccosh}\left(\frac{X}{X_p}\right) \\ &= \exp\left(\frac{1}{2}X_p^2\right) \ln\left\{\frac{X}{X_p} + \left[\left(\frac{X}{X_p}\right)^2 - 1\right]^{1/2}\right\}, \end{aligned} \quad (9)$$

which is needed to start the solution. For large X it is easy to show that $Y \approx X$, a result that corresponds to the familiar condition for the emergent ray at the refraction angle, namely,

$$\sin^2 \theta_{ex} = \frac{n_p}{n_c}, \quad (10)$$

where n_p is the electron density at the perigee and θ_{ex} is the angle the ray makes with the y (laser) axis on exit.

Rays that are emitted nonparallel to the axis are included in this description in one of two ways.

(1) Rays emitted at an angle θ to the axis at density n and in the direction of decreasing gradient have the extrapolated perigee density given by

$$n_p = n \cos^2 \theta + n_c \sin^2 \theta. \quad (11)$$

If the value of this term exceeds the central density n_0 the perigee does not exist. However, the integration may proceed from X with $\exp(-X_p^2)$ given by the value of Eq. (11) in Eq. (8).

(2) For rays emitted at an angle $-\theta$ to the axis, against the direction of decreasing density, the integration is taken from the emission point X to the perigee using Eq. (11) and thence further. If the perigee does not exist, the integration is taken to the axis, and thence forward.

Henceforward we shall consider only rays emitted at their perigee.

Figure 3(a) shows the variation of the path length at $X = 10$ for different starting points. We note that there is a minimum path at about $X_p \approx 0.3$. This is a result of the point of inflection in the density profile at $X = \sqrt{2}$, which allows rays further out to be less refracted. Taking this into account, a good approximation for the ray path for large X is given by $Y = X + \ln(0.9/X)$ for $X_p \leq 0.1$, which takes account of the initial logarithmic form and the limit $Y \sim X$.

However the path length is not a useful term for our purposes. We require the gain length. Assuming that $n_0 \ll n_c$ and that in the density region of interest $G \approx G_0 n_e/n_0$ where G_0 is the gain at the maximum, the gain length is

$$\begin{aligned} &\sqrt{\frac{n_c}{n_0}} G_0 x_1 \int_{X_p}^{\infty} \frac{\exp(-X^2)}{\sqrt{[\exp(-X_p^2) - \exp(-X^2)]}} dX \\ &\approx \sqrt{\frac{n_c}{n_0}} G_0 x_1 (0.0491 - 1.006 \ln X_p), \end{aligned} \quad (12)$$

the approximation being valid for $X_p \leq 1.2$, beyond which the gain length is small.

We may use these results [Fig. 3(b)] to estimate the refraction length [15], namely, the effective length of the plasma before refraction limits further amplification, by calculating the value of Y at which the gain length is 0.9 times its final value. We also identify the value of X at this point as the refraction width. For positions within the $1/e$ width of the maximum, we find values of Y ranging from 6 for the strongest rays to about 1 for the weaker. The equivalent width is about 0.5. This enables us to identify a limiting length of plasma which can be used effectively, namely, $\sim 6\sqrt{n_c/n_0}(x_1)$. For a tantalum laser operating at 45 \AA in plasma at 10^{22} cm^{-3} of width $x_1 \approx 5 \mu\text{m}$, the refraction length is 6 mm, and suggests that only short plasma lengths of about 5 mm should be used. Lower-density or larger plasmas would increase this limit. For this configuration the output beam will be emitted at an angle of about 14 mrad to the laser axis. We note that, for plasma of these dimensions, only a very small fraction of the rays will be emitted near the axis at sufficiently small angles to pass through the plasma end face.

F. Slabs or Foils?

Figure 4 compares the energy required to generate the conditions for Cu-like ionization for a 100 $\mu\text{g}/\text{cm}^2$ foil and a slab for varying atomic number. It can be seen that at atomic number ~ 73 the foil becomes more efficient. It can also be seen that mass from the slab exceeds that of the foil at $Z \approx 68$.

Foils in principle have significant advantages over slabs for our purposes, but to take advantage of these will require careful design.

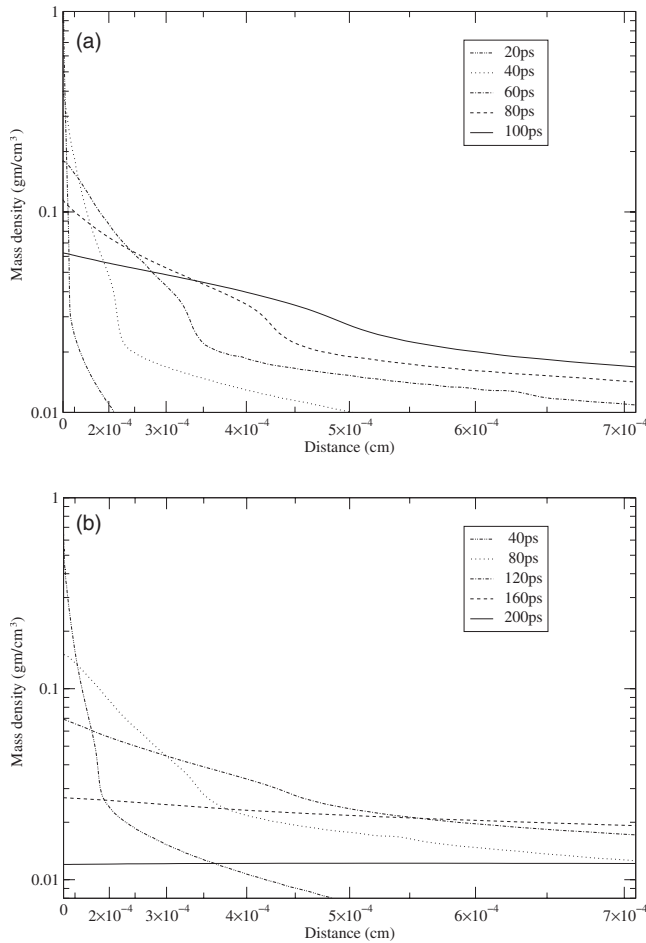


FIG. 5. Logarithm of the mass density in an exploding foil plotted as a function of the square of the expansion distance, so that a Gaussian profile appears as a straight line. (a) Pulse 225 J/cm and 100 ps duration. (b) Pulse 213 J/cm and 200 ps duration.

- (1) The total plasma mass is controlled.
- (2) The electron density in the usable region can be high.
- (3) The density profile of the exploding foil is approximately Gaussian, i.e., has a flat top.
- (4) At high density the foil is not transparent and the absorptivity will be matched to slabs.

However, to set against these advantages there are drawbacks.

(1) Kinetic energy is equipartitioned with thermal, so that a larger fraction of energy is used to drive the expansion than with slabs.

(2) Timing is critical. The rapid disassembly of the foil must not take place before either the core is hot or the ionization complete.

(3) The foils are thin and easily damaged and the plasma dimensions small. It is critical that plasma expansion maintain the reflective symmetry about the axial plane. Laser beams must be matched.

To take advantage of these properties, we must ensure that the burn and ionization times are short compared to the foil expansion time, and this will determine the prepulse duration to be used.

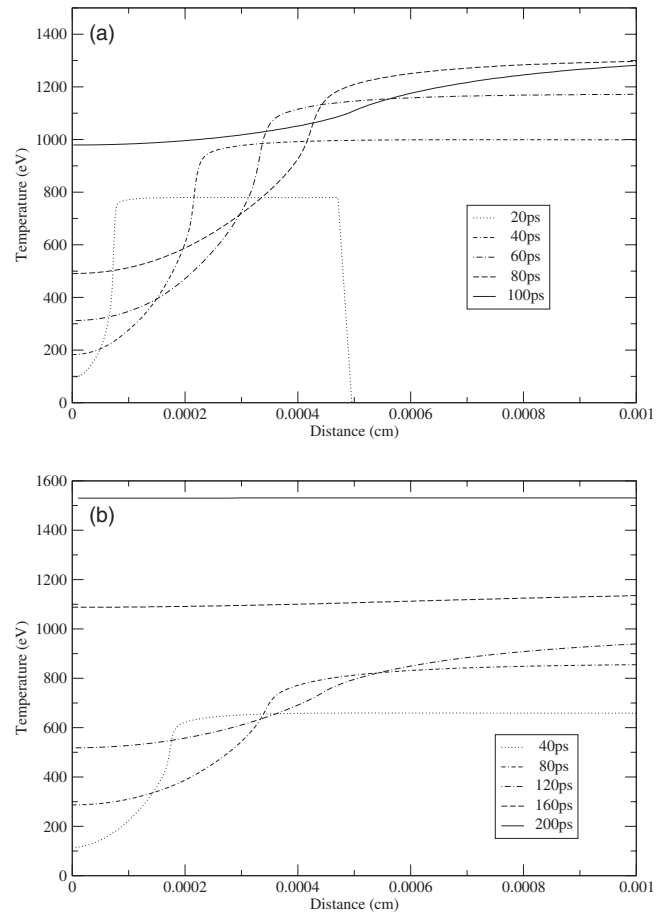


FIG. 6. Temperature in an exploding foil plotted as a function of the expansion distance. (a) Pulse 225 J/cm and 100 ps duration. (b) Pulse 213 J/cm and 200 ps duration.

III. SIMULATION OF FOIL SYSTEMS

We now turn to a series of simulation experiments whose role is to examine the validity of our simple models. We consider a tantalum foil of appropriate mass (usually 100 $\mu\text{g}/\text{cm}^2$) heated by a prepulse of constant power of specified duration and subsequently by a 2 ps main pulse of Gaussian profile and 2100 J/cm² energy density. The foil width is arbitrary but a value of 100 μm was used. The critical surface reflectivity was taken to be 0.7 and the flux limiting factor 0.1, the same values as in paper II.

Figure 5(a) shows the development of the density profile of a 100 $\mu\text{g}/\text{cm}^2$ tantalum foil as a function of time during the 100 ps prepulse required to achieve Cu-like ionization. It is clear that the self-similar hydrodynamic model is a poor approximation. This is a consequence of the fact that the isothermal structure of the plasma is not well established, particularly in the early stages of heating [Fig. 6(a)]. Comparing this sequence with the equivalent longer pulse, 200 ps [Fig. 5(b)], we can see that with the latter a much better Gaussian profile is established by the end of the pulse. Indeed, by about 160 ps the profile is nearly Gaussian. Nonetheless, the exploding foil model does give a useful approximation for the overall energy balance in the form used above.

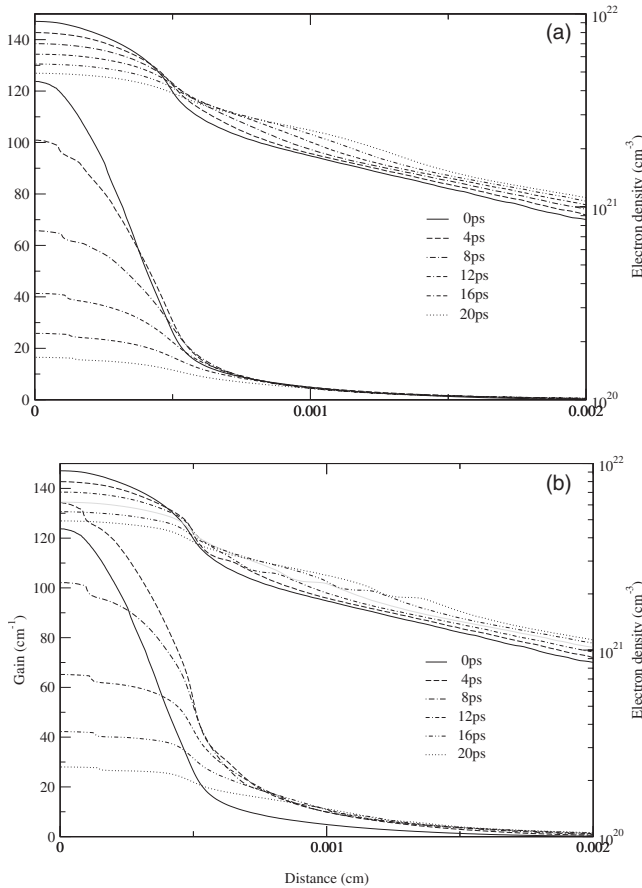


FIG. 7. Gain and density in exploding foils plotted as functions of the expansion distance for different times. (a) No main pulse. (b) Main pulse 2100 J/cm^2 and 2 ps duration.

However, if we compare the central mass density at the end of the prepulse in the two cases, we find a value of 0.062 g/cm^3 for the 100 ps case, compared with 0.012 g/cm^3 for 200 ps. Using the values of energy taken from the simulation, the self-similar model Eq. (7) predicts densities of 0.022 and 0.011 g/cm^3 at the termination of the 100 and 200 ps pulses, respectively. Thus the shorter pulse gives significantly greater central density than the model, whereas the longer pulse has assumed a self-similar density.

This behavior is clearly reflected in the temperature profiles (Fig. 6) during heating. In each case the heat front can be seen clearly. The downstream edge of the front moves outwards convected by the expansion of the foil, a consequence of the heating of the foil at its center. In the 100 ps case it can be seen that, even at the end of the pulse, the core plasma is not yet isothermal, whereas in the 200 ps case the temperature is uniform after 160 ps. In each case the temperature is sufficient to ensure that the plasma has ionization ~ 44 , corresponding to the Cu-like stage. It will be noted that the peak temperature attained at the end of the longer heating pulse (1520 eV) is significantly higher than with the shorter pulse (1280 eV), despite the fact that the input energies are almost equal, a difference accentuated at the center in the latter case by the failure to achieve uniformity. The reason for this is the lower absorption with the short pulse (60%) compared with (82%), due to the shorter plasma expansion fan with the former.

TABLE I. Irradiance parameters to achieve Cu-like ionization in $100 \mu\text{g/cm}^2$ foils with different pulse lengths.

Pulse length (ps)	Density (cm^{-3})	Temperature (eV)	Input (J/cm^2)	Absorbed (J/cm^2)
100	9.1×10^{21}	979	17200	10380
125	5.4×10^{21}	1260	16840	11870
140	4.8×10^{21}	1119	14380	10940
175	2.8×10^{21}	1278	14560	12010
200	1.5×10^{21}	1530	16490	13880

Table I shows the central density and temperature achieved by pulses of varying duration and energy which achieve Cu-like ionization. Although the net input energy is almost constant, it can be seen that there is a weak minimum in the energy requirement at about 150 ps as the increased absorption is balanced by the increasing thermal burn and ionization times. The temperature at the center is correspondingly increased as the pulse length increases. However, the dominant feature is the strong decrease in the central density with pulse length.

Since the gain scales strongly with density (Fig. 2), the marked advantage of using a short prepulse can be seen: although this must be balanced against the stronger effects of refraction due to the higher density. This enables us to benefit not only from the density time scaling Eq. (7), but also from the delay taken to establish the self-similar profile and yet have a nearly isothermal plasma at the termination of the pulse. Further shortening of the pulse, however, is not satisfactory, as the ionization is limited by the time available at the temperature achieved at the center of the foil, and the density profile at the center is less favorable.

A. Gain development

Comparing the temperatures generated at the center in Table I with those required in Fig. 2 for good gain generation, we see that, even with the shortest pulses, no further heating is required to generate significant gain. The temperature at the end of the 100 ps prepulse is 979 eV, compared to the minimum 750 eV required for ionization, the additional temperature ensuring that the Cu-like ionization was achieved. Figure 7 compares the gain history achieved with no main pulse and that with one of 2100 J/cm^2 in 2 ps, time

TABLE II. Gain achieved at end of prepulse and at maximum.

Pulse length (ps)	Prepulse gain (cm^{-1})	Peak gain (cm^{-1})	Density (cm^{-3})
100	124.8	134.9	9.14×10^{21}
125	59.45	66.36	5.38×10^{21}
140	44.09	60.93	4.78×10^{21}
175	18.95	25.94	2.79×10^{21}
200	9.342	10.25	1.43×10^{21}

TABLE III. Output values obtained with 2100 J/cm² main pulse.

Pulse length (ps)	Gain length	Energy (μ J)	Deflection (mrad)	Divergence (mrad)	Gain (cm ⁻¹)	Effective length (cm)	Half-width (ps)
100	22.0	77.5	14.2	2.8	58.4	0.38	4.0
125	18.2	39.1	9.6	5.7	43.5	0.42	8.7
140	18.1	39.3	7.6	7.6	43.2	0.42	9.9
175	9.9	0.08	1.9	3.7	22.1	0.45	3.3

being measured from the end of the prepulse, i.e., at the start of the main pulse.

It can be seen that without the main pulse the peak gain value 123 cm⁻¹ occurs at the end of the prepulse, as is to be expected. On the other hand, the gain increases after the short main pulse has finished, up to a value of 134 cm⁻¹. More marked is the wider distribution of gain and the longer lifetime with the main pulse. In both cases the gain zone is contained within the relatively flat density peak.

Table II shows the gain at the start of the main pulse and the peak gain for a range of prepulse durations corresponding to the prepulse energies given in Table I and a main pulse of 2100 J/cm². It can be seen that as the prepulse duration is increased the gains are markedly reduced, and the difference between the peak gain with and without the main pulse is proportionately larger. With the main pulse the peak gain occurs at approximately 4 ps in every case. However, compensating for the reduced gain, the longer pulses have a density profile with significantly smaller gradient.

The results are readily understood in terms of the dynamics of the foil expansion and the inversion discussed earlier. Thus the longer pulse produces a more nearly self-similar density profile with small central density at the end of the prepulse. The gain is therefore correspondingly reduced approximately proportionately. The reduction of the central density peak by expansion leads to a gentler density gradient.

For a 100 μ g/cm² tantalum foil, we conclude from these results that the pulse should not be longer than about 150 ps. Heavier foils will allow correspondingly longer pulses, but also require increased energy; for example, a 167 μ g/cm² tantalum foil will work satisfactorily with a 200 ps pulse, but requires absorbed energy 1.74×10^4 J/cm² instead of 1.04×10^4 J/cm²—an increase approximately proportional to the mass. However, the laser energy delivered is significantly reduced from this scaling, namely, 2.1×10^4 J/cm² compared to 1.7×10^4 J/cm², due to improved absorption in a longer-scale-length coronal plasma with the heavier foil. The pulse length, 200 ps in this case, is slightly too short to fully match our model as the temperature profile at the completion of the prepulse is similar to that shown in Fig. 6(a) where the plasma is not isothermal: in consequence the peaks of the ionization and gain at the center are delayed. Nonetheless, the peak electron density is nearly 10²² cm⁻³ and, after a main pulse of 2.8×10^4 J/cm², the gain of value 132 cm⁻¹ is comparable to that obtained from the thinner foil. However, the radial width is larger, allowing a longer gain path against refraction.

B. Output estimates

In order to identify the effect of refraction, which from our earlier analysis is expected to be significant, we have

carried out a number of ray-tracing simulations using the profiles discussed in the previous section over a plasma length of 5 mm. These were carried out using the code RAYTRACE described in paper II, modified to calculate the ray averages using the saturated power. The results of these calculations are summarized in Tables III and IV for the two cases of additional main pulse heating and none, respectively. The values tabulated are the averages taken over the x-ray laser pulse weighted by the output power, as would be measured in an experiment. The gain, gain length, and energy are straightforward values obtained from the averaging. The pulse width is the full width at half maximum (FWHM) of the output power temporal signal. The output comprises two distinct beams, one on each side of the axis defined by the planes containing the pump pulse and the foil. The deflection and divergence are measured with respect to the axis, the former being the angular deviation of the center of the beam and the latter the FWHM spread. The effective length is the average length of the ray paths over which gain is active, essentially the refraction length. As may be expected the values are dominated by those at the times at maximum gain length.

Turning to the case with a 2100 J/cm² main pulse, some points are immediately apparent. The 100 ps prepulse heating yields the largest gain, gain length, and total output energy, as would be expected from the high density at which gain is achieved. It can be seen that, in this case, the effective plasma length is limited to less than 5 mm by the refraction in the plasma, as estimated by our earlier calculation. We therefore restricted our calculations to 5 mm, as noted earlier. Trial calculations at 10 mm did not show marked increase in signal except for the long prepulse, where the rays are weakly refracted. This, however, is not an efficient method of improving the signal. The amplification at prepulse duration less than 140 ps is saturated in each case. We note the close similarity in the values at 125 and 140 ps as both the gain and the path length are nearly equal. In every case the deflection angles are consistent with the perigee on axis. The angular spread of the beam increased as the density decreased, allowing a greater range of initial ray conditions to make a substantial contribution.

The same general features are shown when no main pulse is applied. Clearly the gains are reduced and the output correspondingly diminished. Nonetheless, significant output is achieved for the shorter prepulse. However, in this case the 140 ps prepulse plasma yields significantly less output than the 125 ps one. In fact, the output in the two cases is noticeably different in detail. As can be seen, the 125 ps case is strongly deflected by refraction, in contrast to the 140 ps

TABLE IV. Output values obtained without main pulse.

Pulse length (ps)	Gain length	Energy (μJ)	Deflection (mrad)	Divergence (mrad)	Gain (cm^{-1})	Effective length (cm)	Half-width (ps)
100	20.0	23.3	11.8	4.5	51.2	0.39	4.7
125	17.1	14.3	9.0	9.0	39.4	0.43	6.8
140	16.4	8.1	3.8	9.2	36.7	0.44	3.3
175	5.9	0.003	2.4	4.3	14.1	0.42	2.1

pulse. We note that these differences are much less marked when the main pulse is applied: since the two cases are just at the borderline of saturation, slight changes of the gain length make large changes in the energy associated with particular rays. We note the markedly increased beam divergence without the main pulse, consequent to the strongest beam paths being less well defined due to weaker amplification. Very weak output is calculated from the 175 ps pulse, resulting from low gain due to low density.

IV. DISCUSSION

The main thrust of this work has been to demonstrate the feasibility of laser-irradiated thin foils as a medium for developing short-wavelength soft x-ray laser radiation. In previous work, we showed that slabs provide a suitable medium down to wavelengths of about 50 Å, when the energy and temperature needed to support the necessary Ni-like ion stage become prohibitive. By restricting the mass of the target, these quantities can be bounded against the increasing mass of plasma heated by thermal and radiative conduction. However, in order to maximize the operating density, we have found that the primary heating pulse (prepulse) should be of limited duration (about 100 ps). As the pulse duration is increased, the central density falls and the gain decreases. For a tantalum foil of mass 100 $\mu\text{g}/\text{cm}^2$, a pulse of 100 ps is suitable, but increasing the mass of the foil to 167 $\mu\text{g}/\text{cm}^2$ requires an increase to 200 ps and a corresponding increase in pump energy. In this work, we have assumed that the prepulse has a square temporal (and spatial) profile. In practice, a rapid rise and sharp fall greatly improve the pumping by allowing the plasma to form in the correct ionization state at high density. Moving to a Gaussian temporal profile reduces the density and thus the available gain.

The central problem with short-wavelength x-ray lasers based on collisionally pumped Ni-like ions is the high electron temperature required to achieve the necessary ionization. As we have found, this is sufficient to achieve reasonably strong gain without additional pumping, provided the central density is high. However, a significant improvement in performance is obtained by additional short-pulse pumping (Tables III and IV), due to the increased temperature generated by the second (main) pulse. As this pulse is short it allows the plasma to rapidly heat before further ionization or expansion sets in, which would reduce both the inversion and gain, as earlier suggested by MacGowan *et al.* [6].

If we compare the values required to ionize the plasma to the Cu-like stage given in Table I with those in Fig. 4, we see

that the analytic scaling gives a value of $8.5 \times 10^3 \text{ J}/\text{cm}^2$ compared to $1.04 \times 10^4 \text{ J}/\text{cm}^2$ from the simulation. Of the difference, $1.05 \times 10^3 \text{ J}/\text{cm}^2$ is accounted for by radiation emitted from the plasma; the remainder is due to the increased temperature required to achieve the ionization during the pulse. Less than half this radiation is re-absorbed in the dense upstream plasma, and gives rise to additional heat conduction by radiation transport. However, the EHYBRID code does not include this effect, which is small for short pulses, but, as can be seen from Table I, increases with the pulse length.

Refractive loss from the gain region is a serious problem for these high-density systems. Operating at high density gives high gain, but the beam is strongly deflected and the ray path length limited. To this end it may be preferable to relax the prepulse duration to values larger than those for peak gain to obtain a less tightly conditioned system (e.g., 150 instead of 100 ps for 100 μg foil). At these high gains these systems are expected to be strongly saturated even for the limited path lengths allowed. In an earlier work [15], we examined the effects of saturation on lasers whose total length exceeded that allowed by refraction. In principle, we must expect that the signal variation predicted there may occur, but is unlikely to be observed or to present any serious problem as the proposed lengths are about equal to the refraction length.

Exploding foils formed the basis of the successful x-ray laser designs developed at Livermore in the late 1980s. One of the most important of these early designs used tantalum foils lased at 45 Å [6]. Using the NOVA laser system as pump, these devices lacked the flexibility in pump source required to optimize the gain and output as suggested here. The experiments used a 167 $\mu\text{g}/\text{cm}^2$ foil heated by a single pulse of length 500 ps, suggesting that the foil would have expanded to quite low density when lasing was established; a result confirmed by the consistent length scaling up to 2 cm. The energy density on the foil, $\sim 2 \times 10^5 \text{ J}/\text{cm}^2$, was substantially larger than the $2 \times 10^4 \text{ J}/\text{cm}^2$ value estimated by our model; this difference is accounted for by radiation loss, the spatial and temporal profiles of the beam, and the gain occurring during the rising edge of the pulse. The results are not inconsistent with the picture presented here.

ACKNOWLEDGMENTS

It is a pleasure to acknowledge useful conversations with Professor G. J. Tallents. This work could not have been carried out without the availability of the atomic data code obtained from R. D. Cowan at Los Alamos.

- [1] G. J. Pert, Phys. Rev. A **73**, 033809 (2006).
- [2] G. J. Pert, Phys. Rev. A **75**, 023808 (2007).
- [3] D. L. Matthews, P. L. Hagelstein, M. D. Rosen, M. J. Eckart, N. M. Ceglio, A. U. Hazi, H. Medeck, B. J. MacGowan, J. Trebes, B. L. Whitten *et al.*, Phys. Rev. Lett. **54**, 110 (1985).
- [4] B. J. MacGowan, S. Maxon, P. L. Hagelstein, C. J. Keane, R. A. London, D. L. Matthews, M. D. Rosen, J. H. Scofield, and D. A. Whelan, Phys. Rev. Lett. **59**, 2157 (1987).
- [5] B. J. MacGowan, S. Maxon, C. J. Keane, R. A. London, D. L. Matthews, and D. A. Whelan, J. Opt. Soc. Am. B **5**, 1858 (1988).
- [6] B. J. MacGowan, S. Maxon, L. B. DaSilva, D. J. Fields, C. J. Keane, D. L. Matthews, A. L. Osterheld, J. H. Scofield, G. Shimkaveg, and G. F. Stone, Phys. Rev. Lett. **65**, 420 (1990).
- [7] B. J. MacGowan, L. B. DaSilva, D. J. Fields, A. R. Fry, C. J. Keane, J. A. Koch, D. L. Matthews, S. Maxon, S. Mrowka, A. L. Osterheld *et al.*, in *X-ray lasers 1990*, edited by G. J. Tallents, IOP Conf. Proc. No. 116 (Institute of Physics, Bristol, 1990), pp. 221–230.
- [8] R. Smith, G. J. Tallents, J. Zhang, G. Eker, S. McCabe, G. J. Pert, and E. Wolfrum, Phys. Rev. A **59**, R47 (1999).
- [9] R. Fabbro, C. Max, and E. Fabre, Phys. Fluids **28**, 1463 (1985).
- [10] R. A. London and M. D. Rosen, Phys. Fluids **29**, 3813 (1986).
- [11] G. J. Pert, Laser Part. Beams **5**, 643 (1987).
- [12] I. V. Nemchinov, Prikl. Mekh. Tekh. Fiz. **5**, 18 (1964).
- [13] A. Caruso and R. Gratton, Phys. Fluids **11**, 839 (1969).
- [14] R. A. London, Phys. Fluids **31**, 184 (1988).
- [15] G. J. Pert, Opt. Commun. **236**, 173 (2004).